ARCHIVES OF ELECTRICAL ENGINEERING VOL. 69(2), pp. 433–453 (2020)

DOI 10.24425/aee.2020.133036

Intermittent power smoothing control for grid connected hybrid wind/PV system using battery-EDLC storage devices

N.S. JAYALAKSHMI [1], D.N. GAONKAR[2], R.P. KARTHIK[3], P. PRASANNA[4]

[1]*Department of Electrical and Electronics Engineering*
Manipal Institute of Technology
MAHE, Manipal, INDIA-576104, India

[2]*Department of Electrical and Electronics Engineering*
NITK, Surathkal, Karnataka, India

[3]*Department of Electrical and Electronics Engineering*
Vidya Vikas Institute of Engineering and Technology
India

[4]*Associate Quality Assurance Engineer, Oracle India Private Limited*
Bangalore, India-560 025
e-mail: jayalakshmi.ns@manipal.edu

(Received: 21.11.2018, Revised: 27.01.2020)

Abstract: Wind and solar radiation are intermittent with stochastic fluctuations, which can influence the stability of operation of the hybrid system in the grid integrated mode of operation. In this research work, a smoothing control method for mitigating output power variations for a grid integrated wind/PV hybrid system using a battery and electric double layer capacitor (EDLC) is investigated. The power fluctuations of the hybrid system are absorbed by a battery and EDLC during wide variations in power generated from the solar and wind system, subsequently, the power supplied to the grid is smoothened. This makes higher penetration and incorporation of renewable energy resources to the utility system possible. The control strategy of the inverter is realized to inject the power to the utility system with the unity power factor and a constant DC bus voltage. Both photovoltaic (PV) and wind systems are controlled for extracting maximum output power. In order to observe the performance of the hybrid system under practical situations in smoothing the output power fluctuations, one-day practical site wind velocity and irradiation data are considered. The dynamic modeling and effectiveness of this control method

are verified in the MATLAB/Simulink environment. The simulation results show that the output power variations of the hybrid wind/PV system can be significantly mitigated using the combination of battery and EDLC based storage systems. The power smoothing controller proposed for the hybrid storage devices is advantageous as compared to the control technique which uses either battery or ultracapacitor used for smoothing the fluctuating power.

Key words: energy storage devices, inverter controller, MPPT controller, power smoothing, PV system, wind power

1. Introduction

Due to the ever-growing energy consumption and the rapid exhaustion of resources of fossil fuels, the need for utilizing renewable energy sources has increased in recent years. To meet the present-day demand for electrical power, both wind and solar power systems are found to be the prominent renewable power generation technologies. However, the power produced by wind and PV systems is highly reliant on environmental conditions. The growing penetration of these intermittent renewable energy resources is the main challenge for traditional distribution networks. The unpredictable and intermittent power output of wind and PV power systems can impact negatively on the grid integrated operation of the hybrid system. For effective smoothing of the power, energy storage devices are used which can provide and absorb power during fluctuations. Many research papers present the power smoothing methods using a single storage device like the battery which causes a reduction in the life of the battery. Hence, this work focuses on the enhancement of the life of storage devices by using a hybrid energy storage system.

The combination of wind and PV power systems to the utility grid is not adequate to fulfill the requirements of quality of power [1]. In [2], the power smoothing is achieved by means of the battery storage system alone for a PV based distributed generation system using a simple moving average based capacity optimization method. In [3], the performance of the hybrid storage system in a microgrid with AC and DC buses is presented. In this work, both battery and ultracapacitor are used as the storage system. The control method of the storage devices is designed considering voltage at a DC link. In [4], the supercapacitor bank is used for power managing of a DC-coupled wind/hydrogen hybrid power system. Energy storage systems are significant for a grid integrated system. The oscillations in power by the wind-solar hybrid system are smoothened by using storage devices. The unpredicted and oscillated power profile of hybrid PV and wind energy systems may lead to fluctuations in frequency as well as voltage. Conventionally battery-based storage devices are used to compensate for the output power variations in wind and solar-based power generations [5]. The battery system can be used to enhance the quality of generated power and the transient stability of a wind farm [6]. Recently EDLC based storage systems are used in several research articles for renewable energy applications. The EDLC has lower energy density and unlimited cycling capability compared to the battery with higher energy density and limited cycling [7, 8]. Therefore, supercapacitors are ideal for short-term storage that enables wind turbine generators to mitigate the fast changes in power output [9]. In a doubly-fed induction generator design, the EDLC energy storage device is integrated in order to smoothen out the output from

the wind power generation system [10]. A Kalman filter-based power smoothing method for a PV and wind-based power system with a battery is proposed in [11]. An ultracapacitor based power smoothing technique for a grid-tied PV/wind hybrid system is presented in [12]. The average of the total power produced by renewable sources is used to compute the reference power.

Many research articles discuss the control performance of the battery or EDLC storage device used for power smoothing of either individual wind or PV generation system. In this paper, to lower the stress of a battery and to improve battery lifetime, EDLCs are used. This work focuses on increasing the use of renewable sources by hybridizing PV and wind systems and smoothing their power output based on the demand by using hybrid energy storage devices. The battery provides power during long term power variations and the EDLC bank supports during the power fluctuations for a very short time, but they are relatively expensive. Both power sources and energy storage devices are connected to a common DC bus and then integrated into the utility system through a single 3-phase inverter. The controller designed for the inverter is able to inject smoothed total real power to the utility and to keep the DC bus voltage constant. A novel control scheme for power smoothing of the grid integrated hybrid wind/PV system using a battery-EDLC storage system has been proposed. In [12], the power fluctuations are reduced for the PV-wind hybrid system using only the ultracapacitor bank. This paper presents the improvements to the power smoothing controller presented in [12], by distributing the power fluctuations among the hybrid energy storage system comprising a battery and EDLC bank. When a combination of the battery and EDLC is used in the system, the power stress on individual storage devices is minimized. The EDLC bank can handle sudden power fluctuations. The coordinated voltage control at DC link and storage devices is proposed for smoothing the output power of the system. To observe the performance of the system under real scenarios, data for the speed of the wind and solar irradiation collected for 24 hours are considered. Also, this control scheme provides required smooth power in accordance with the grid requirement. The final result of the proposed control strategy is a smooth power output that can be injected into the grid.

2. Structure of the proposed system and modeling

Fig. 1 shows the grid-integrated DC-coupled hybrid power generation system (HPGS) with a battery and EDLCs. Both sources and energy storage devices are integrated into a DC link and then coupled to the utility through a 3-phase inverter. The battery and EDLC storage devices are entrenched in the DC bus with the use of DC–DC bidirectional converters. A novel control strategy is developed for DC–DC converters of battery and EDLC systems for supplying smoothened power to the grid from the wind/PV hybrid system. The wind system considered in this paper uses the permanent magnet generator due to its high-power factor and high efficiency. It also results in a smaller size, minimum weight and higher torque to size ratio. The maximum power point tracking (MPPT) controllers exploit the maximum possible power from both PV and wind energy systems at any operating condition. The controller designed for the inverter helps to inject power to the grid at the unity power factor (UPF) and regulates DC link voltage for different operating conditions.

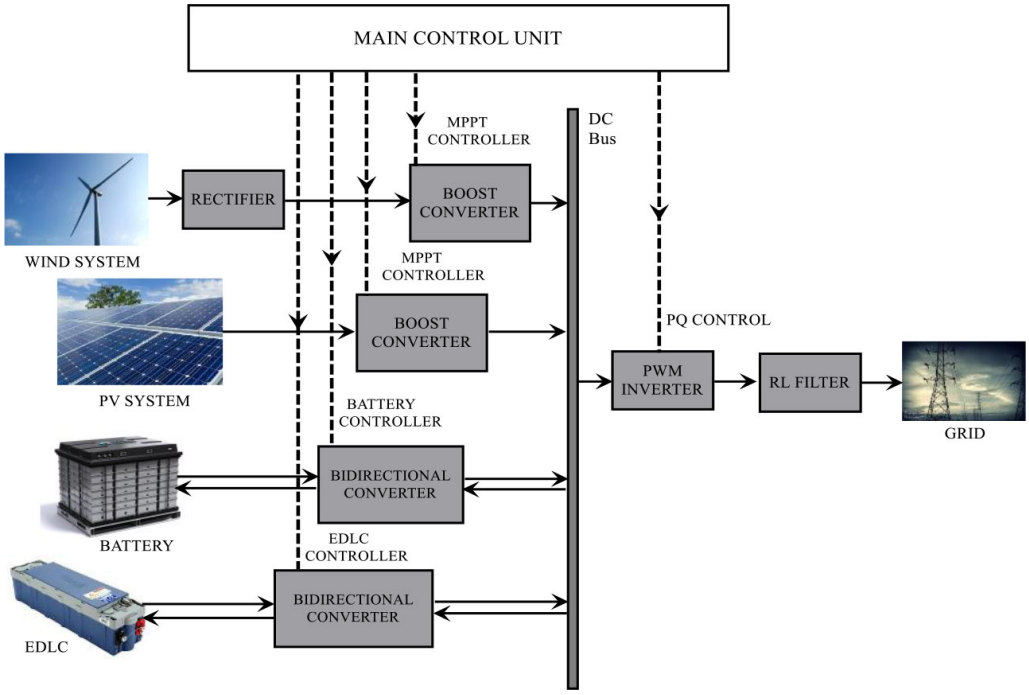

Fig. 1. Schematic diagram of the DC-coupled hybrid power generation system

2.1. Modeling of the wind generation system

The wind generating system uses a wind turbine with a permanent magnet synchronous generator (PMSG), a 3-phase uncontrolled rectifier and a boost converter with an MPPT controller. The power available from a turbine [13] is

$$P_m = \frac{1}{2}\rho A V_w^3 C_p(\lambda\beta), \tag{1}$$

where: P_m is the power in watts, V_w is the velocity of wind in m/s, A is the rotor swept area, ρ is the density of air, C_p is the coefficient of performance. The tip speed ratio (TSR) is represented by

$$\lambda = \frac{\omega_m R}{V_w}, \tag{2}$$

where: ω_m is the rotor speed in rad/s, R is the blade radius in meters. The rated wind power generation is 20 kW. The voltage equations for v_d and v_q of the PMSG are given by [14].

$$v_d = R_s i_d + L_d \frac{\mathrm{d}i_d}{\mathrm{d}t} - \omega L_q i_q, \tag{3}$$

$$v_q = R_s i_q + L_q \frac{\mathrm{d}i_q}{\mathrm{d}t} + \omega L_d i_d + \omega \phi_m, \tag{4}$$

where: ω is the angular frequency, R_s is the stator winding resistance; i_d and i_q are the d and q axis machine currents; ϕ_m represents the flux linkages; L_d and L_q are, respectively the inductances corresponding to the d-axis and q-axis.

If the rotor is cylindrical, the torque equation is expressed as:

$$T_e = \frac{3}{2} p \phi_m i_{qs}\,, \tag{5}$$

where p is the pole pairs. The circuit model of the PMSG is depicted in Fig. 2.

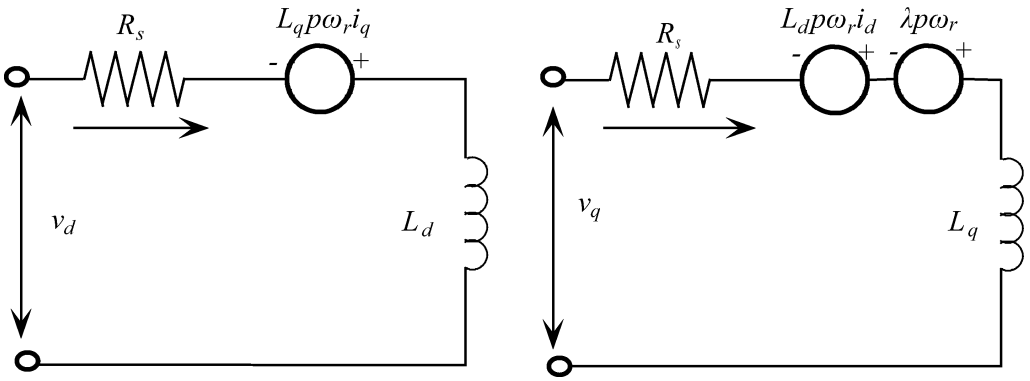

Fig. 2. Circuit model of the PMSG

2.2. PV system modeling

The total power generation from the PV system is 40 kW. The photocurrent I_{ph} is given by [15].

$$I = N_p I_{ph} - N_p I_s \left\{ e^{\frac{q}{AkT}\left(\frac{V}{N_s} + \frac{IR_s}{N_p}\right)} - 1 \right\} - \frac{N_P}{R_{sh}} \left(\frac{V}{N_s} + \frac{IR_s}{N_p} \right), \tag{6}$$

where: the normal diode current is I_o; N_s and N_p are the number of PV cells connected in parallel and series respectively; R_s and R_{sh} are the equivalent series and shunt resistance.

2.3. Modeling of EDLC bank

The lead-acid battery is taken for the study and its equivalent circuit is represented in Fig. 3(a). The controlled source is described in the following equations [21, 16]:

$$V_{\text{batt}} = E_{\text{batt}} - R_{\text{batt}} I_{\text{batt}}\,, \tag{7}$$

where: E_{batt} is the no-load voltage (V); I_{batt} is the battery current (A); V_{batt} is the battery terminal voltage (V); R_{batt} is the internal resistance of the battery (Ω). The EDLC is embedded into the DC bus via a DC–DC converter.

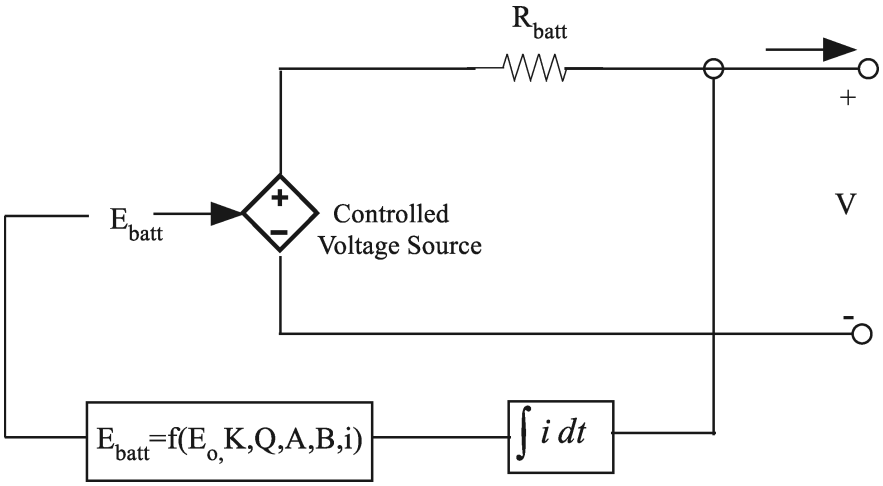

(a)

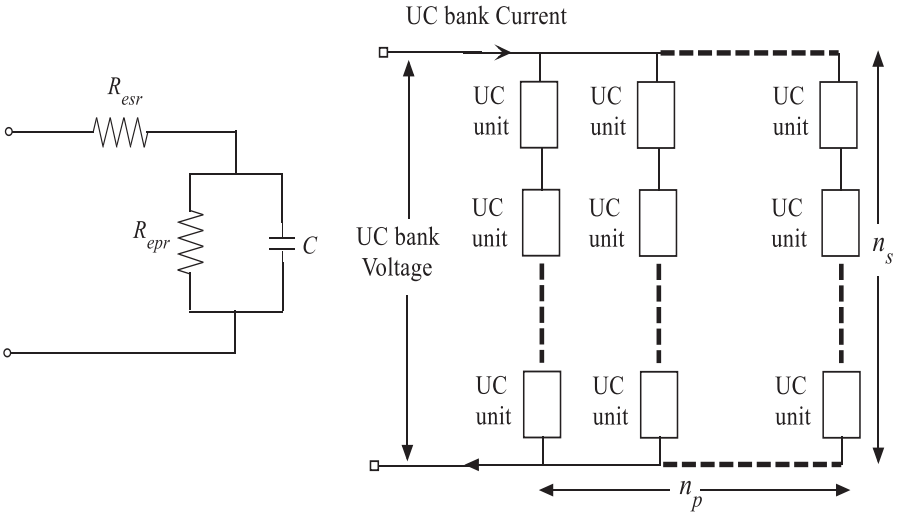

(b)

Fig. 3. Equivalent electrical circuit of battery and UC bank: electrical circuit of battery (a); classical equivalent circuit model of UC (b)

For the simulation study, the Maxwell Boostcap PC2500 ultracapacitor unit is chosen. Each unit has a voltage of 2.5 V (2700 F capacity). The minimum and maximum voltages are 400 V and 600 V, respectively.

Let $E_{\max}$ be the maximum stored energy and E_{inst} be the instantaneous stored energy of an ultracapacitor (UC), the percentage state of charge (SOC) is determined using the following

expressions.

$$E_{\max} = 0.5C\,(V_{\max})^2 \qquad \text{and} \qquad E_{\text{inst}} = 0.5C\,(V_{\text{inst}})^2\,, \tag{8}$$

$$\%\text{SOC} = \frac{E_{\text{inst}}}{E_{\max}} \times 100. \tag{9}$$

The UC voltage and current are necessary to be monitored according to the following limits.

$$V_{\min} < V < V_{\max} \qquad \text{and} \qquad I_{Ch,\max} < I < I_{Dis,\max}\,, \tag{10}$$

where: $V_{\min}$ and $V_{\max}$ are the minimum and maximum working voltage and $I_{Ch,\max}$ and $I_{Dis,\max}$ are the maximum charging and discharging current of the UC. Fig. 3(b) shows the connection of the UC units to form a UC bank that is proficient in providing the required amount of power. The overall resistance and capacitance of the UC bank are determined as:

$$R_{uc\,\text{total}} = n_s \frac{R_{esr}}{n_p}\,, \tag{11}$$

$$C_{uc\,\text{total}} = n_p \frac{C}{n_s}\,. \tag{12}$$

The EDLC bank with a string of 240 units is connected in series. The power in the EDLC can be given as below,

$$P_{edlc}(t) = P_{pv}(t) + P_{\text{wind}}(t) - P_{\text{smooth}}(t) \pm P_b(t). \tag{13}$$

In this research work, the battery and EDLC bank are controlled to absorb the discrepancy between the total generated power from the wind/PV hybrid system at any operating condition and the smooth power is supplied to the utility system. The Maxwell Boostcap PC2500 ultracapacitor unit parameters [17, 18] are reported in Table 1.

Table 1. Parameters of the system under study

Turbine	Radius of blade = 3.7 m; air density = 1.225 Kg/m^2; $C_{p\,\max}$ = 0.47; number of blades = 3
PMSG	Resistance of stator per phase = 0.1764 Ω; $L_d = L_q$ = 4.35 mH; torque constant = 13.91 N-m/A peak; $V_{w\text{rated}}$ = 12 m/s; P_{out} = 20 kW; pole pairs = 18; inertia = 0.205 Kg·m^2
PV arrays	k = 1.38e^{-23}; n = 1.2; N_S = 32; NP = 21; q = 1.6e^{-19}; V_g = 1.12; V_{oc} = 21.1 V; I_{sc} = 3.8 A; G = 1000 W/m^2; P_{out} = 40 kW
EDLC	600 V; initial SOC = 60%; 11.25 F; unit cell = 2.5 V; N_s = 240
Battery	600 V; initial SOC = 80%; N_s = 300; N_p = 64; capacity = 420 Ah
DC link voltage:	780 V; DC link capacitor = 5000 μF
Grid parameters:	415 V; 50 Hz; X/R ratio = 7
Filter:	R = 2 mΩ; L = 250e^{-6} H

3. Control schemes for power electronic devices

This section discusses the MPPT controllers used for wind and PV systems, control strategy employed for battery and EDLC bank as well as the active/reactive power (PQ) control method for the inverter.

3.1. MPPT controllers

The shaft torque of the wind turbine is represented by [13]:

$$T_m = \frac{P_m}{\omega_m} = \frac{1}{2}\rho\pi R^5 \frac{\omega_m^3}{\lambda^3} C_p(\lambda, \beta). \tag{14}$$

The power coefficient C_p is retained at its maximum value using the MPPT algorithm and corresponding to λ_{opt} power coefficient $C_p = C_{p\,\max}$. The maximum power output is given by:

$$P_m = 0.5\rho A C_{p\,\max} \left(\frac{R\omega_{\text{ref}}}{\lambda_{\text{opt}}}\right)^3, \tag{15}$$

where ω_{ref} is given by the expression:

$$\omega_{\text{ref}} = \frac{V_w \lambda_{\text{opt}}}{R}. \tag{16}$$

The turbine reference speed ω_{ref} is produced by the MPPT algorithm using the P and O method. For PV arrays, the incremental conductance method is used and at the point of maximum power [19], $\mathrm{d}P/\mathrm{d}V = 0; \therefore \mathrm{d}I/\mathrm{d}V = -I/V$. A proportional-integral controller reduces the error between negative conductance and incremental conductance.

3.2. Control strategy for battery and EDLC bank

The battery performance can be improved in terms of the power density by combining EDLCs with batteries which are typically low power devices with high power density. Fig. 4 shows the control strategy for a battery and EDLC bank in detail. Two DC–DC bidirectional converters are considered for connecting the battery and EDLC bank to the DC link. Since DC voltage at a common bus is controlled by the control scheme of the grid side converter, the control scheme of bidirectional converters is used for the power flow regulation of storage devices. The bidirectional converters consist of insulated-gate bipolar transistor (IGBT) switches T_1, T_2 and T_3, T_4 respectively. By controlling their duty ratios the currents of storage devices can be controlled. The duty ratio D_1 of switch T_2 or T_4 in buck mode can be given as:

$$D_1 = \frac{V_b \text{ or } V_{sc}}{V_{dc}}. \tag{17}$$

The duty ratio D_2 of switch T_1 or T_3 in boost mode is $D_2 = 1 - D_1$. The current control strategy has two control loops. The sum of powers produced from the wind and PV system is matched with reference power signal and the difference is fed to a PI controller which generates references of current signals for the storage devices. The current references $I_B{}^*$ and $I_{\text{EDLC}}{}^*$ are

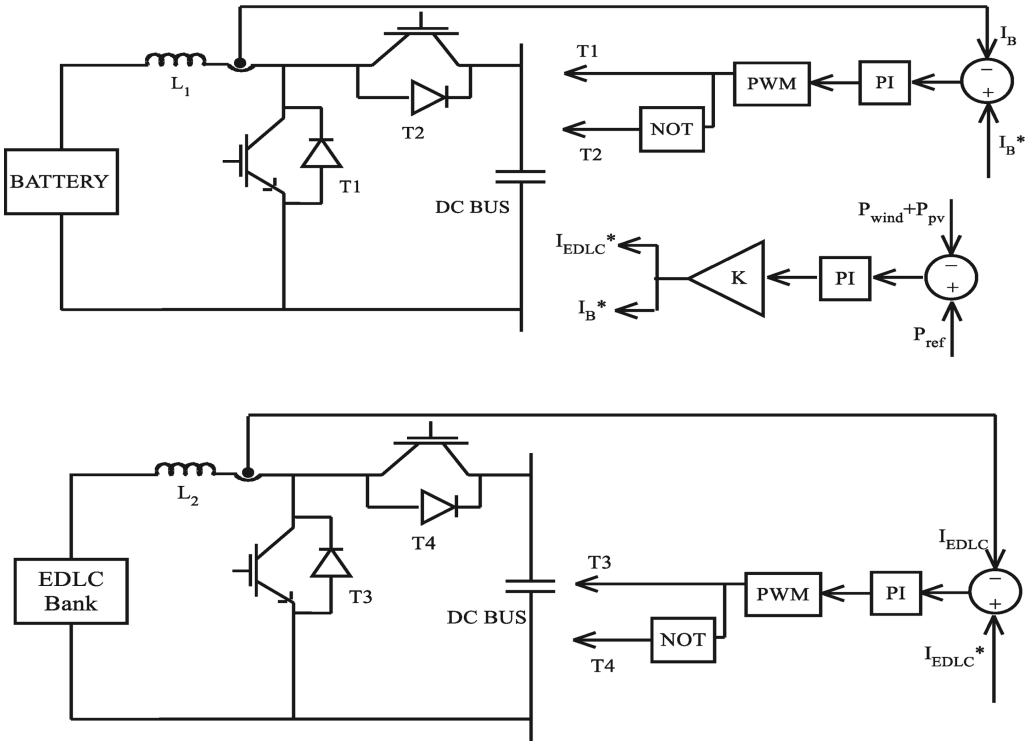

Fig. 4. Control strategy for battery and EDLC bank

further compared with the battery and EDLC currents which form the inner current loops to generate pulses to the bidirectional DC–DC converters. If the reference power exceeds the total generated power, the converters act in boost mode and this power difference is supplied by storage devices. If the actual power exceeds the power reference signal, the converters act in buck mode thereby charging storage devices. In this work, for achieving equal load sharing among storage devices, the gain factor K is taken as 0.5. In Fig. 4, I_B and I_{EDLC} are battery and EDLC currents, respectively. This helps in power-sharing among the storage devices and reducing the power stress on individual storage devices. The transfer functions of DC–DC converters of the battery and EDLC bank are:

$$\frac{\hat{i}_b}{\hat{d}} = \frac{3.39 \times 10^5 (s + 20)}{s^2 + 10s + 5.14 \times 10^4}, \tag{18}$$

$$\frac{\hat{i}_{uc}}{\hat{d}} = \frac{86667(s + 20)}{s^2 + 10s + 13.1 \times 10^4}. \tag{19}$$

The Bode diagram for DC–DC converters of the battery and EDLC bank are shown in Fig. 5(a) and Fig. 5(b), respectively.

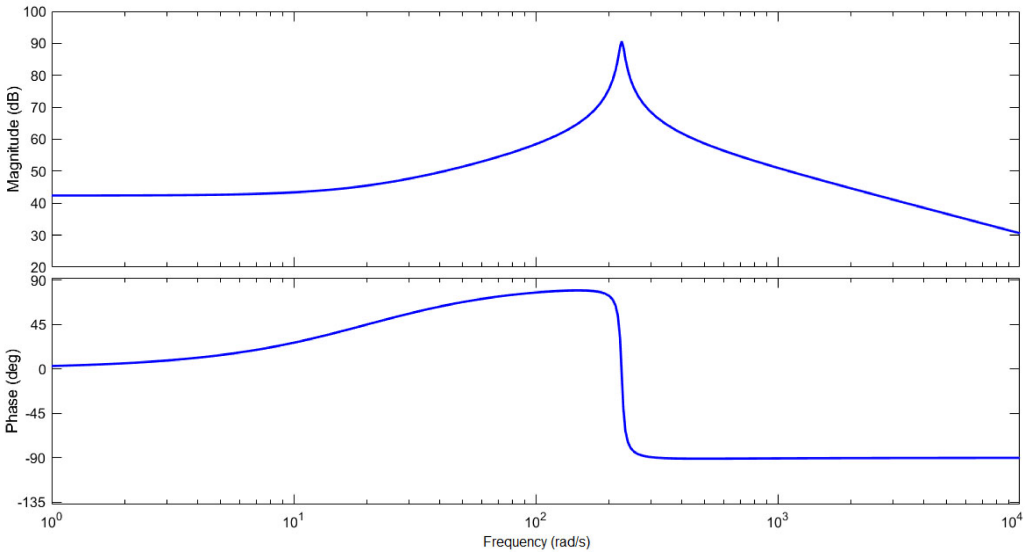

(a)

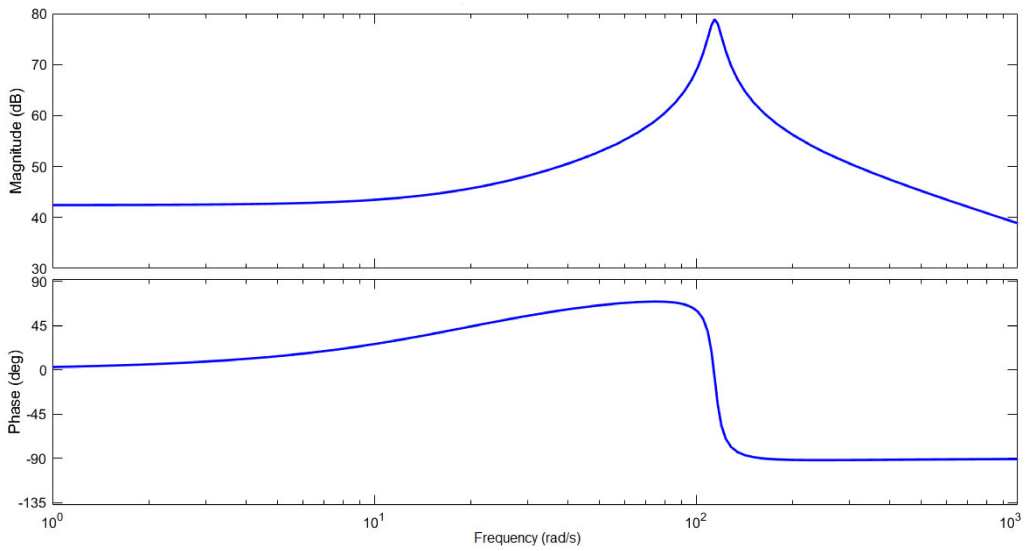

(b)

Fig. 5. The Bode diagram for DC–DC converter of storage devices: battery bank (a); EDLC bank (b)

3.3. PQ control strategy for inverter

The instantaneous power is given by:

$$p(t) = v_a i_a + v_b i_b + v_c i_c \,. \tag{20}$$

Since

$$V_g = V_{gd} + j0,$$

the real power and reactive power expressions are:

$$P = 1.5\left(V_{gd} i_d\right) \qquad \text{and} \qquad Q = 1.5\left(V_{gd} i_q\right). \tag{21}$$

The real power and reactive power injected to the grid are regulated by governing the d and q-axis currents i_d and i_q respectively. There are two control loops in the control system: an outer loop that maintains the DC bus voltage at 780 V and inner control loops which control i_d and i_q. The control signal obtained from the outer control loop is used to create a current reference of d-axis for controlling the injected active power [20]. To transfer only active power to the grid, the $i_q = 0$ and the schematic of the inverter controller is shown in Fig. 6.

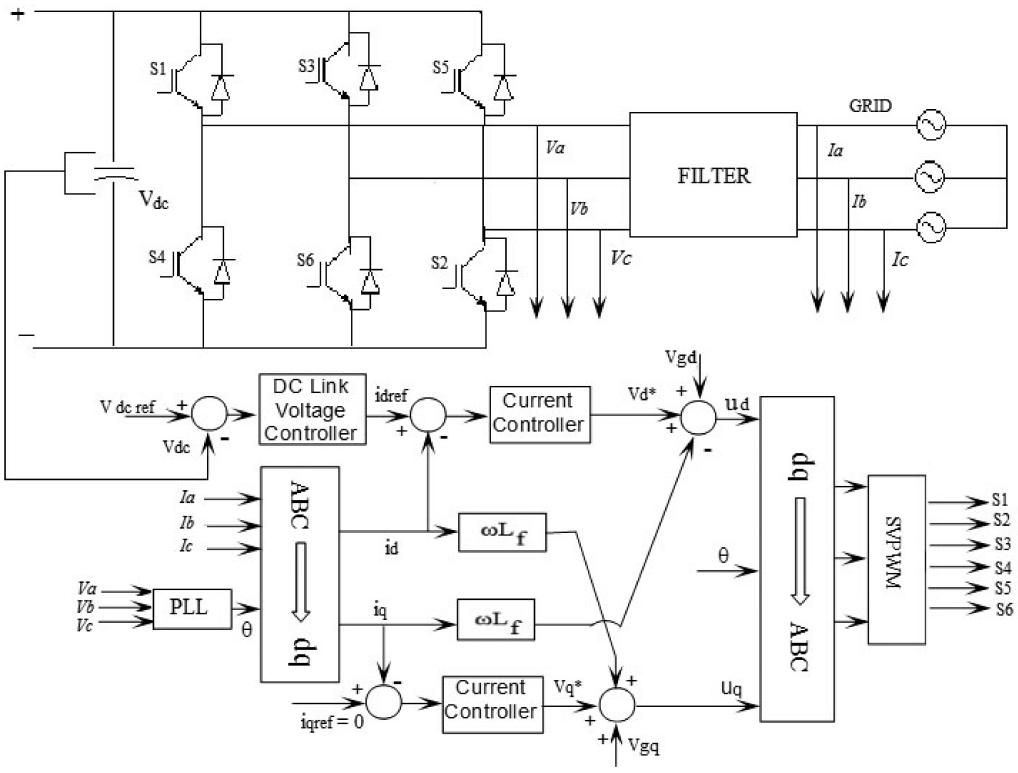

Fig. 6. Schematic of inverter control strategy

4. Simulation results and discussions

The storage systems are coupled to the DC bus using two bidirectional DC-DC converters. The hybrid system is integrated with the grid via a three-phase inverter and R-L filters. The simulation is done by considering the practical site data for wind speed and solar irradiation for

one day [22, 23] and scaling it down to 4.8 s. The parameters of the studied system are reported in Table 1. The parameters of the PI controllers for different controllers are given in Table 2.

Table 2. Parameters of PI controllers

PV arrays MPPT controller:	$K_p = 500$, $K_i = 0.0001$
PMSG MPPT controller:	$K_p = 0.3$, $K_i = 0.0001$
EDLC bank:	$K_p = 0.045$, $K_i = 1.5$
Battery bank:	$K_p = 0.015$, $K_i = 1.5$
DC-link voltage regulator:	$K_p = 7$, $K_i = 800$
Inverter d-axis current controller:	$K_p = 0.3$, $K_i = 20$
Inverter q-axis current controller:	$K_p = 0.3$, $K_i = 20$

Case 1: Generation of constant reference output power from the hybrid system

In this case, the power supplied by the hybrid system to the utility grid is constant. Fig. 7(a) and Fig. 7(b) represent the wind speed and solar irradiation profile respectively for 24 hours. Fig. 8 represents the total wind and PV power produced during the one-day period. The wind power generation is high during night time. Also, the PV systems generate power only during the day time with huge variations. To evaluate the power smoothing achieved using the proposed control scheme, highly intermittent data of wind speed and irradiation are considered for analysis. The variations in the output power of PV and wind energy systems will affect the stability of the grid. Hence power injected to the grid should be smoothened.

The output power of the battery and EDLC bank are reported in Fig. 9(a) and Fig. 9(b) respectively. The battery supplies a maximum power of 11 kW during the lowest power generation

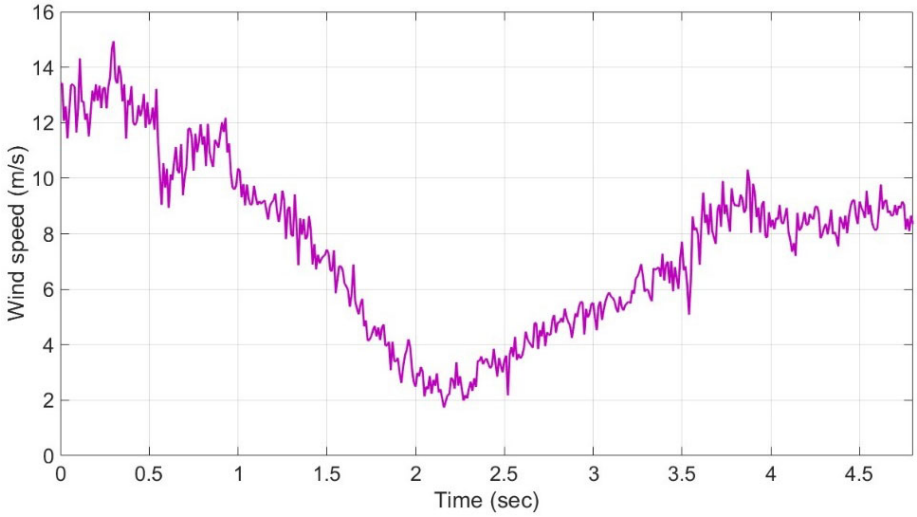

(a)

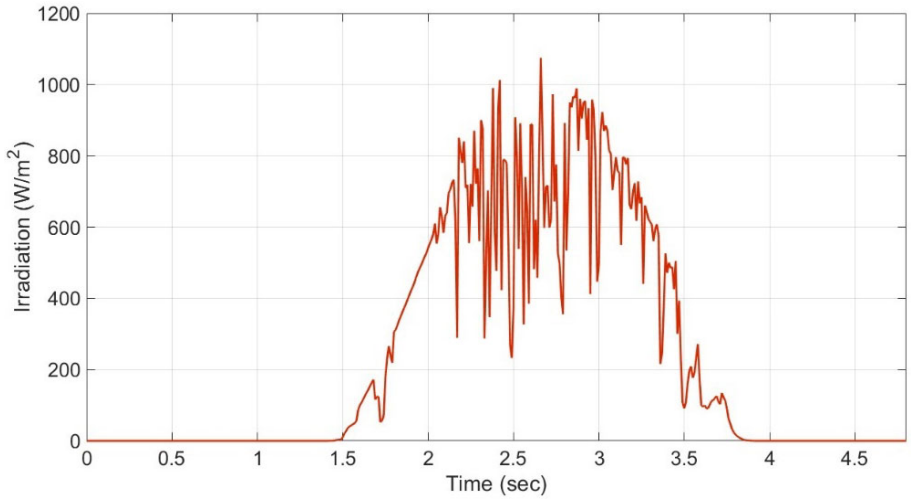

(b)

Fig. 7. Wind speed profile and solar irradiation profile for one day: wind speed profile (a); solar irradiation profile (b)

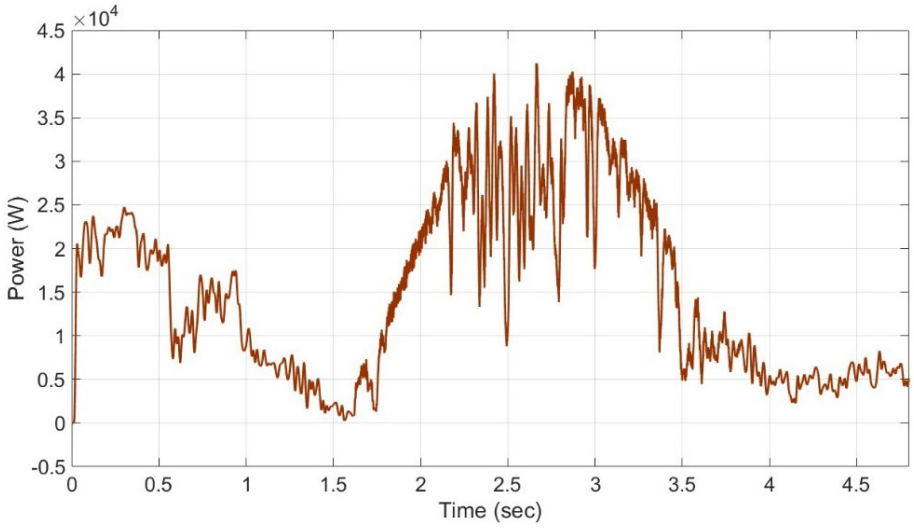

Fig. 8. Total wind and solar power generations

period. Then the battery absorbs a maximum of 8 kW during the peak power generation. The SOC of the battery and EDLC bank are reported in Fig. 10(a) and Fig. 10(b) respectively. Most of the transient power is supplied by the EDLC in the beginning and it will supply a maximum power of 11 kW and absorbs a maximum of 8 kW. Therefore, it is observed from the simulations that both the battery and EDLC supply or absorb the power difference. The voltage across the battery and

EDLC bank are shown correspondingly in Fig. 11(a) and Fig. 11(b). Negative power represents charging operation and positive power represents discharging operation. The SOC raises when the storage systems receive the power and it reduces when the power is delivered. Similarly, the voltage drops during discharging operation and it increases during charging.

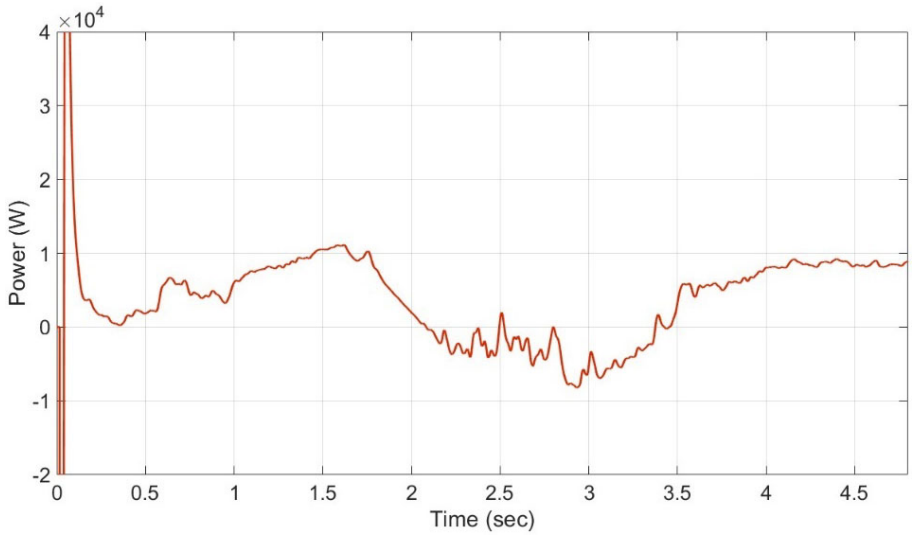

(a)

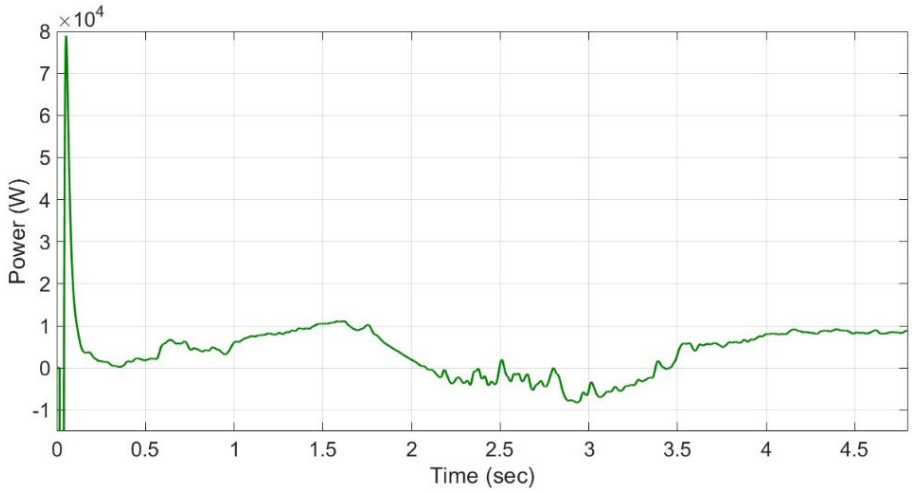

(b)

Fig. 9. Output power of storage devices: battery power (a); EDLC power (b)

Fig. 12 represents total wind and PV power generations and smoothed power injected to the utility grid. Most of the fluctuating powers are supplied or absorbed by storage devices. It can be

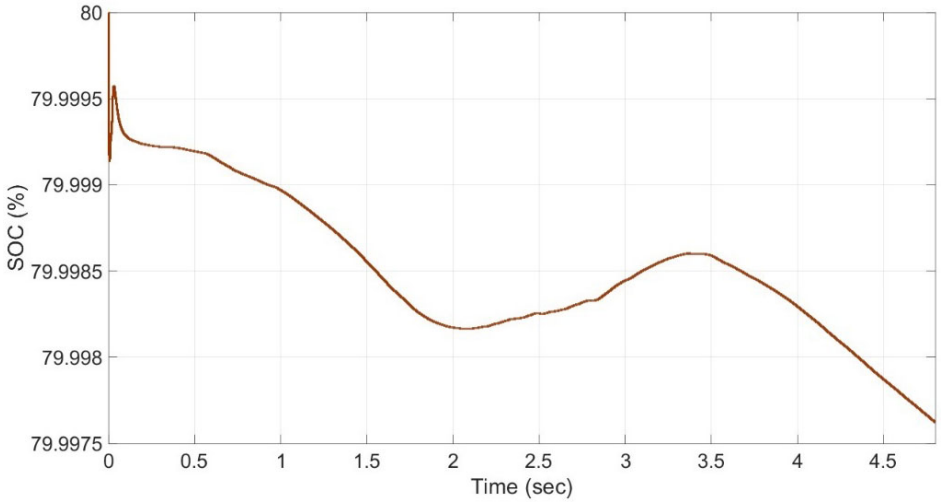

(a)

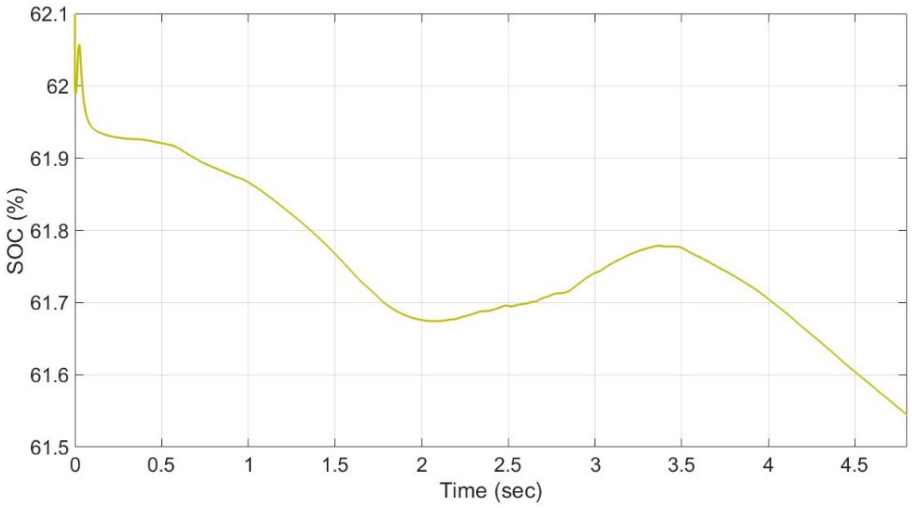

(b)

Fig. 10. SOC of storage devices: SOC of battery (a); SOC of EDLC (b)

realized from Fig. 12 that, the control method proposed could effectively minimize the total wind and PV power fluctuations. Few recent research papers present the power smoothing with a single energy storage system or by modifying the control schemes [2, 11, 12] and [24–26]. This power smoothing controller is more effective as compared to the power smoothening techniques proposed in the literature as this control scheme involves the hybridization of energy storage devices for enhancing the life of the storage system. The same PV-wind hybrid system is analyzed in [12] and smoothening is achieved with an ultracapacitor based on averaging technique. The proposed

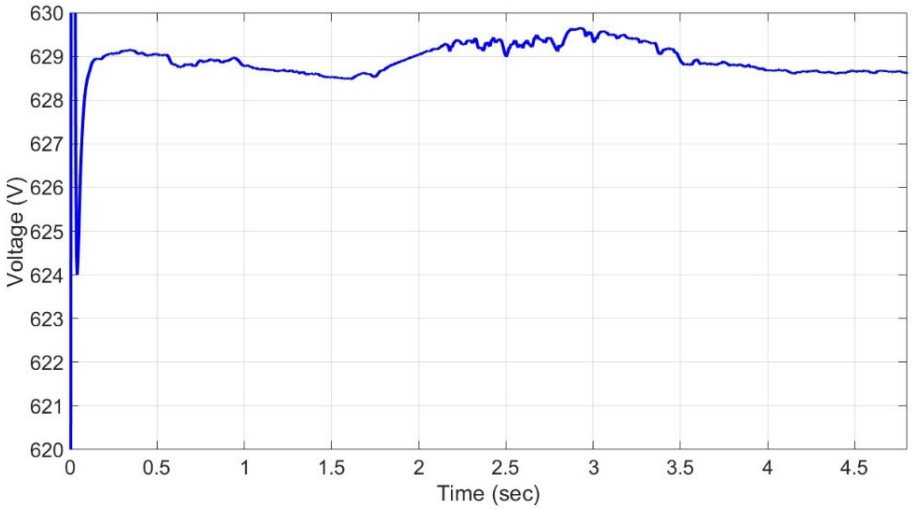

(a)

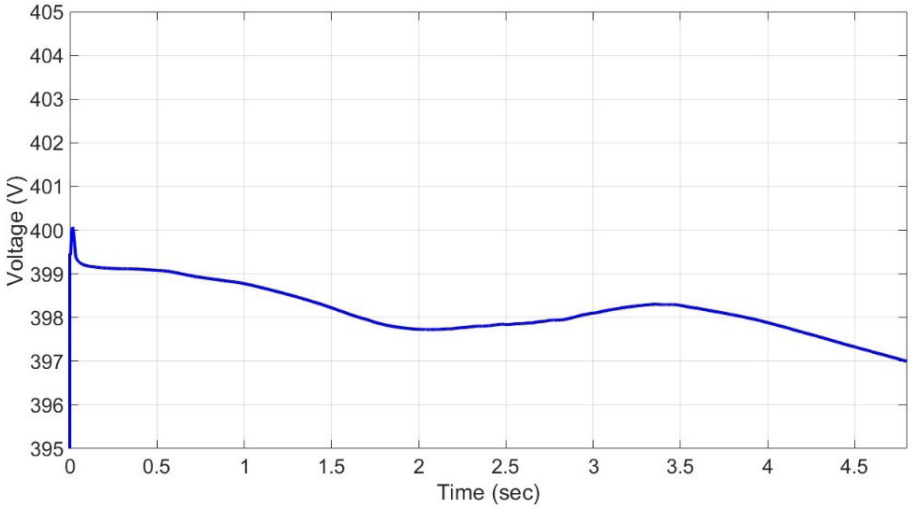

(b)

Fig. 11. Voltage of storage devices: battery voltage (a); EDLC voltage (b)

smoothing controller is more reliable and practical as compared to the one proposed in [12, 16] as the fluctuating power is shared amongst the storage devices and smooth power is supplied to the grid based on the requirements.

Fig. 13(a) shows the variation in DC link voltage. The reference value of V_{dc} chosen is 780 V. The voltage at the DC bus is maintained at 780 V using the inverter controller even during huge variations in power output. Fig. 13(b) shows reactive power supplied by a hybrid power generation system (HPGS) to the utility system. This is zero during fluctuations in the wind and PV power

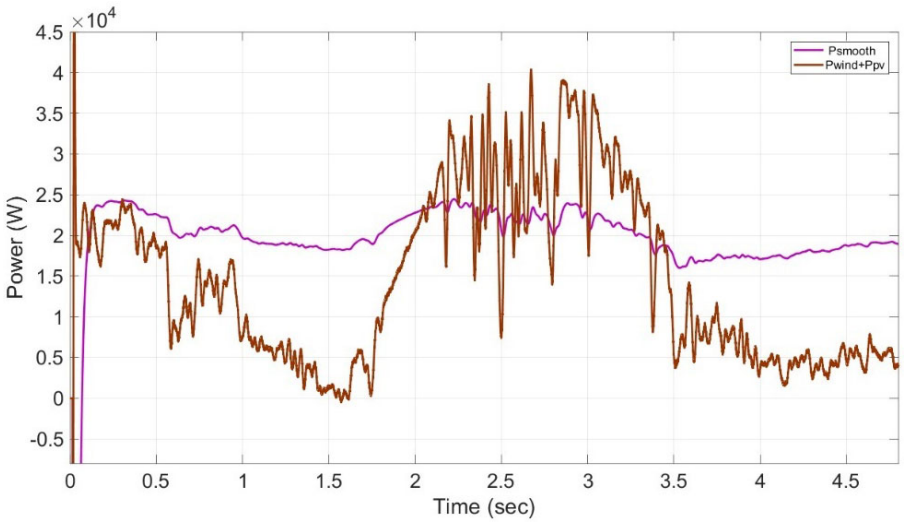

Fig. 12. Total wind-solar power generations and smoothed power injected to the grid

generations. The voltage at the DC bus and power supplied to the utility can be well controlled using the proposed combined battery-EDLC storage devices. It is observed from the results that the grid power can be smoothened due to the operation of the battery and UC bank to extract the fluctuated power from the HPGS. The battery and UC bank are utilized to absorb the fluctuated component of wind/PV power before delivering to the grid during the irradiation and wind speed variations, which improves the grid power quality. Also, due to the presence of both battery and UC bank in the system, the lifetime of the battery system increases as the fluctuating components are shared among both storage devices.

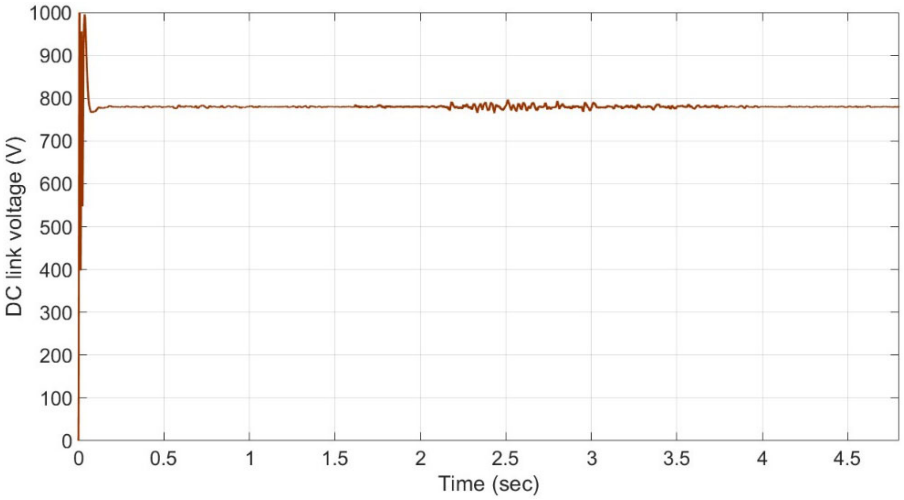

(a)

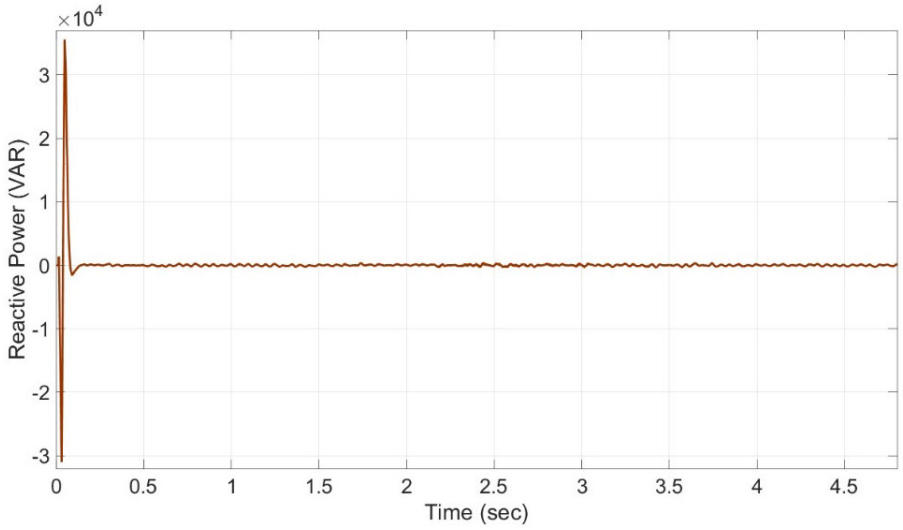

(b)

Fig. 13. DC link voltage and reactive power delivered by the HPGS to the utility system: DC link voltage (a); reactive power (b)

Case 2: Generation of hybrid power output of the system in accordance with the grid codes

In this circumstance, the hybrid system is supplying power to the utility in consensus with the grid codes. Fig. 14 shows responses of reference power and the total power generated by HPGS. It is seen that the HPGS generates power in accordance with the grid requirements. Fig. 15(a) and

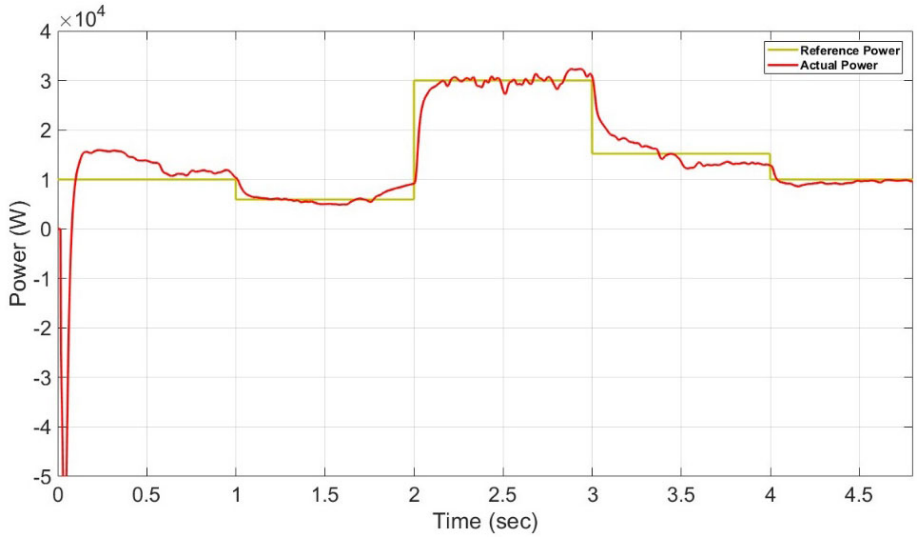

Fig. 14. Variation of reference power and total power generated by hybrid system

Fig. 15(b) show variation in the DC bus voltage and reactive power given by the hybrid system to the grid. The DC bus voltage is well controlled around 780 V even during huge variations in the output power. The reactive power provided by the HPGS to the grid is zero during variations in the power generated and also in reference power depending on the requirement of grid power. This confirms the effectiveness of the control strategy implemented to support power smoothing control and is possible to penetrate higher renewable power to the utility system.

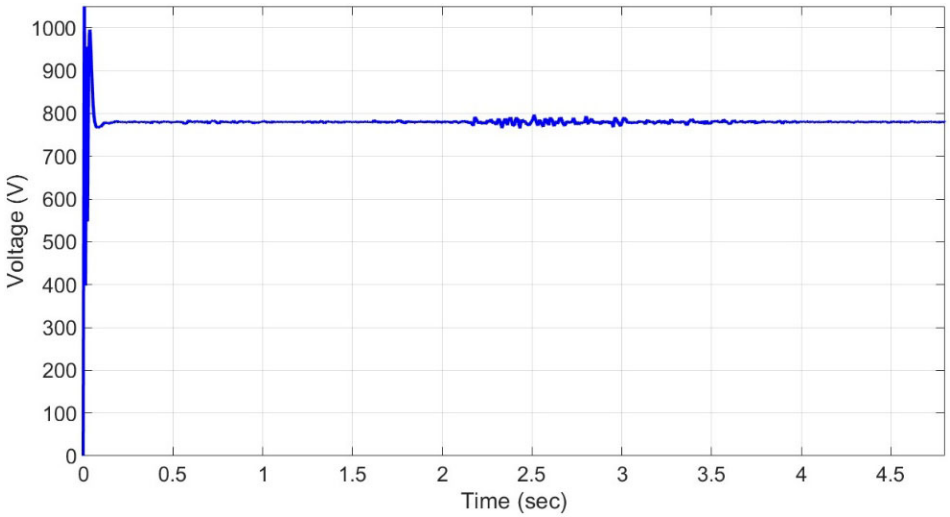

(a)

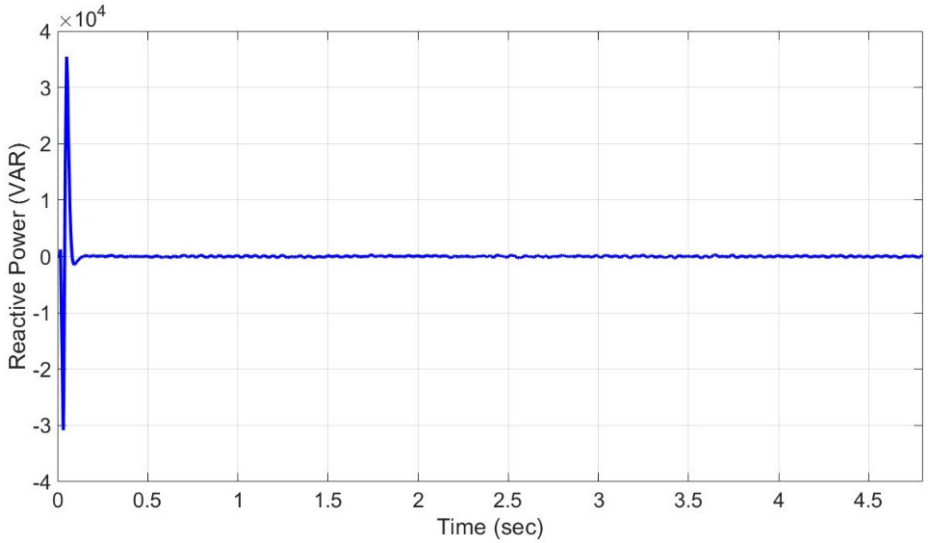

(b)

Fig. 15. DC link voltage and reactive power: DC link voltage (a); reactive power (b)

5. Conclusions

The intermittent power output of the hybrid wind/PV system creates an adverse effect on the operations of the utility grid. One of the means for mitigating these fluctuations is to integrate the hybrid system with battery and EDLC combination with a suitable controller. A detailed dynamic model of the grid-integrated hybrid wind/PV system with the battery and EDLC is implemented in the MATLAB/Simulink environment. Both power sources are controlled to extract their maximum possible power. A current control strategy is developed for smoothing the total power injected into the utility grid. The requirement of maintaining constant DC link voltage is realized while injecting power to the utility grid at a unity power factor. It is found that the proposed method increases the quality of power transferred to the grid even during large fluctuations in the wind and PV power. The combination of the battery and EDLC helps in improving the life of the storage system by sharing the fluctuating power among the devices. Thus an effective smoothing controller is developed for the PV-wind hybrid system using hybrid energy storage devices to supply smooth power to the utility grid based on the requirements.

References

[1] Li X., Li N., Jia X., Hui D., *Fuzzy logic based smoothing control of wind/PV generation output fluctuations with battery energy storage system*, IEEE International Conference on Electrical Machines and Systems (ICEMS), Beijing, China, pp. 1–5 (2011).

[2] Nayak C.K., Nayak M.R., Behera R., *Simple moving average based capacity optimization for VRLA battery in PV power smoothing application using MCTLBO*, Journal of Energy Storage, vol. 17, pp. 20–28 (2018).

[3] Baoquan L., Fang Z., Xianwen B., *Control method of the transient compensation process of a hybrid energy storage system based on battery and ultra-capacitor in micro-grid*, IEEE International Symposium on Industrial Electronics (ISIE), Hangzhou, China, pp. 1325–1329 (2012).

[4] Zhou T., François B., *Energy management and power control of a hybrid active wind generator for distributed power generation and grid integration*, IEEE Transactions on industrial electronics, vol. 58, no. 1, pp. 95–104 (2011).

[5] Fakham H., Lu D., Francois B., *Power control design of a battery charger in a hybrid active PV generator for load-following applications*, IEEE Transactions on Industrial Electronics, vol. 58, no. 1, pp. 85–94 (2011).

[6] Zeng J., Zhang B., Mao C., Wang Y., *Use of battery energy storage system to improve the power quality and stability of wind farms*, IEEE International Conference on Power System Technology, Chongqing, China, pp. 1–6 (2006).

[7] Samson G.T., Undeland T.M., Ulleberg O., Vie P.J., *Optimal load sharing strategy in a hybrid power system based on pv/fuel cell/battery/supercapacitor*, IEEE International Conference on Clean Electrical Power, Capri, Italy, pp. 141–146 (2009).

[8] Kumar S., Ikkurti H.P., *Design and Control of Novel Power Electronics Interface for Battery-Ultracapacitor Hybrid Energy Storage System*, Proceedings of the International Conference on Sustainable Energy and Intelligent Systems (SEISCON), Chennai, India, pp. 20–22 (2011).

[9] Abbey C., Joos G., *Supercapacitor energy storage for wind energy applications*, IEEE Transactions on Industry Applications, vol. 43, no. 3, pp. 769–776 (2007).

[10] Muyeen S.M., Shishido S., Ali M.H., Takahashi R., Murata T., Tamura J., *Application of energy capacitor system to wind power generation*, Wind Energy, vol. 11, no. 4, pp. 335–350 (2008).

[11] Lamsal D., Sreeram V., Mishra Y., Kumar D., *Smoothing control strategy of wind and photovoltaic output power fluctuation by considering the state of health of battery energy storage system*, IET Renewable Power Generation, vol. 13, no. 4, pp. 578–586 (2019).

[12] Jayalakshmi N.S., Gaonkar D.N., *A new control method to mitigate power fluctuations for grid integrated PV/wind hybrid power system using ultracapacitors*, International Journal of Emerging Electric Power Systems, vol. 17, no. 4, pp. 451–461 (2016).

[13] Slootweg J.G., De Haan S.W., Polinder H., Kling W.L., *General model for representing variable speed wind turbines in power system dynamics simulations*, IEEE Transactions on Power Systems, vol. 18, no. 1, pp. 144–151 (2003).

[14] Chinchilla M., Arnaltes S., Burgos J.C., *Control of permanent-magnet generators applied to variable-speed wind-energy systems connected to the grid*, IEEE Transactions on Energy Conversion, vol. 21, no. 1, pp. 130–135 (2006).

[15] González-Longatt F.M., *Model of photovoltaic module in Matlab*, Ii Cibelec, pp. 1–5 (2005).

[16] Sharma R., Suhag S., *Supercapacitor utilization for power smoothening and stability improvement of a hybrid energy system in a weak grid environment*, Turkish Journal of Electrical Engineering and Computer Sciences, vol. 26, no. 1, pp. 347–362 (2018).

[17] *Ultracapacitor: Parameters*, available at: http://www.maxwell.com/.

[18] Uzunoglu M., Alam M.S., *Dynamic modeling, design, and simulation of a combined PEM fuel cell and ultracapacitor system for stand-alone residential applications*, IEEE Transactions on Energy Conversion, vol. 21, no. 3, pp.767–775 (2006).

[19] Sabhahit J.N., Gaonkar D.N., Nempu P.B., *Integrated power flow and voltage regulation of stand-alone PV–fuel cell system with supercapacitors*, International Journal of Power and Energy Systems, vol. 37, no. 1 (2017).

[20] Rodríguez P., Pou J., Bergas J., Candela J.I., Burgos R.P., Boroyevich D., *Decoupled double synchronous reference frame PLL for power converters control*, IEEE Transactions on Power Electronics, vol. 22, no. 2, pp. 584–592 (2007).

[21] Tremblay O., Dessaint L.A., Dekkiche A.I., *A generic battery model for the dynamic simulation of hybrid electric vehicles*, IEEE Vehicle Power and Propulsion Conference, Arlington, TX, USA, pp. 284–289 (2007).

[22] http://google.org/pdfs/google_heliostat_wind_data_collection, accessed August 2014.

[23] http://www.nrel.gov/midc/oahuarchive/(data source from the National Renewable Energy Laboratory), accessed August 2014.

[24] Worku M.Y., Abido M.A., *Fault Ride-Through and Power Smoothing Control of PMSG-Based Wind Generation Using Supercapacitor Energy Storage System*, Arabian Journal for Science and Engineering, vol. 44, no. 3, pp. 2067–2078 (2019).

[25] Lee H., Hwang M., Muljadi E., Sørensen P., Kang Y.C., *Power-smoothing scheme of a DFIG using the adaptive gain depending on the rotor speed and frequency deviation*, Energies, vol. 10, iss. 4, pp. 1–13 (2017), DOI: 10.3390/en10040555.

[26] Lin F.J., Lu S.Y., Chao J.Y., Chang J.K., *Intelligent PV Power Smoothing Control Using Probabilistic Fuzzy Neural Network with Asymmetric Membership Function*, International Journal of Photoenergy (2017), DOI: 10.1155/2017/8387909.